Developmental factor IRF6 exhibits tumor suppressor activity in squamous cell carcinomas

Elisabetta Botti[a,1], Giulia Spallone[a,1], Francesca Moretti[a,1], Barbara Marinari[a,1], Valentina Pinetti[a], Sergio Galanti[b], Paolo D'Onorio De Meo[c], Francesca De Nicola[b], Federica Ganci[b], Tiziana Castrignanò[c], Graziano Pesole[d], Sergio Chimenti[a], Luisa Guerrini[e], Maurizio Fanciulli[b], Giovanni Blandino[b], Michael Karin[f,2], and Antonio Costanzo[a,b,2]

[a]Department of Dermatology, University of Rome Tor Vergata, 00133 Rome, Italy; [b]Rome Oncogenomic Center, Regina Elena Cancer Institute, 00128 Rome, Italy; [c]Bioinformatic Centre, CASPUR, 00185 Rome, Italy; [d]Institute of Biomembranes and Bioenergetics of the National Research Council and Department of Biochemistry and Molecular Biology, University of Bari, 70121 Bari, Italy; [e]Department of Biomolecular Sciences and Biotechnology, University of Milan, 20133 Milan, Italy; and [f]Laboratory of Gene Regulation and Signal Transduction, Department of Pharmacology and Cancer Center, University of California at San Diego, La Jolla, CA 92093-0723

Contributed by Michael Karin, July 8, 2011 (sent for review February 9, 2011)

The transcription factor interferon regulatory factor 6 (IRF6) regulates craniofacial development and epidermal proliferation. We recently showed that IRF6 is a component of a regulatory feedback loop that controls the proliferative potential of epidermal cells. IRF6 is transcriptionally activated by p63 and induces its proteasome-mediated down-regulation, thereby limiting keratinocyte proliferative potential. We hypothesized that IRF6 may also be involved in skin carcinogenesis. Hence, we analyzed IRF6 expression in a large series of squamous cell carcinomas (SCCs) and found a strong down-regulation of IRF6 that correlated with tumor invasive and differentiation status. IRF6 down-regulation in SCC cell lines and primary tumors correlates with methylation on a CpG dinucleotide island located in its promoter region. To identify the molecular mechanisms regulating IRF6 potential tumor suppressive activity, we performed a genome-wide analysis by combining ChIP sequencing for IRF6 binding sites and gene expression profiling in primary human keratinocytes after siRNA-mediated IRF6 depletion. We observed dysregulation of cell cycle-related genes and genes involved in differentiation, cell adhesion, and cell–cell contact. Many of these genes were direct IRF6 targets. We also performed in vitro invasion assays showing that IRF6 down-regulation promotes invasive behavior and that reintroduction of IRF6 into SCC cells strongly inhibits cell growth. These results indicate a function for IRF6 in suppression of tumorigenesis in stratified epithelia.

Ovo-like 1(drosophila) | skin cancer | oncogene-induced senescence | HRas | transforming growth factor-β

Tumors can be regarded as organs whose development is tightly regulated by factors that control cell growth and neoangiogenesis and interact with the stroma and connective tissue cells (1). Squamous cell carcinomas (SCCs) represent the most frequent type of cancer worldwide, whose pathogenesis involves activating H-Ras mutations as well as up-regulation of c-Myc, loss of p53 function, and expression of mitogenic and inflammatory cytokines (2, 3). SCC development is strongly modulated by the same factors that control normal tissue development during embryogenesis and organogenesis. An example is shown by the fact that tumor-specific down-regulation of the developmental factor i kappa-B kinase alpha (IKKα) promotes skin carcinogenesis in mice and humans by modulating the sensitivity of cells to the developmental cytokine TGFβ (4–7). It is, therefore, of great importance to study how tumor cells use developmental factors to their own benefit, because such factors may represent optimal targets for blocking abnormal tumor development.

IFN regulatory factor 6 (IRF6) is a member of the IRF family of transcription factors (8), but unlike other IRF family members, it is not involved in IFN gene expression (9). Instead, IRF6 controls craniofacial and skin development (9–11), at least in part by interacting with ΔNp63 (12, 13). *Ikkα* and *Irf6* KO mice display very similar developmental phenotypes, including craniofacial abnormalities, limb development defects, and impaired keratinocyte differentiation (9, 11, 14, 15), suggesting that the two factors may act in the same pathways to control cell proliferation and differentiation during development. Based on these factors, we hypothesized that IRF6 may also function as a tumor suppressor in stratified epithelia and tried to explore the molecular mechanisms mediating this function. In the present study, we provide evidence that IRF6 is repressed by promoter methylation in SCC derived from stratified epithelia. Genome-wide analysis of IRF6 binding regions [ChIP sequencing (ChIP-seq)] coupled with microarray analysis of IRF6-depleted human keratinocytes led us to identify direct IRF6 targets involved in cell adhesion and motility and control of epidermal precursor proliferation. The role of IRF6 as a suppressor of SCC invasiveness and proliferation was confirmed by invasion and colony formation assays.

Results

IRF6 Is Down-Regulated in SCC. IRF6 expression was detected by immunohistochemistry in a panel of 50 SCC sections taken from various tissues and 20 sections from normal noncancerous tissues. IRF6 protein was down-regulated in 71% of SCCs (Fig. 1*A*). The amount of IRF6 was found to correlate with histological stage, the highest in well-differentiated tumors and the lowest in high-grade, poorly differentiated SCCs (Fig. 1*A*). Interestingly, although in normal stratified epithelia, strong nuclear localization of IRF6 was detected in the basal and suprabasal layers, a substantial reduction in nuclear IRF6 staining was observed in SCC sections (Fig. 1*A*). Quantification of nuclear staining revealed a clear correlation between the IRF6 nuclear expression and SCC differentiation (Fig. 1*B*). IRF6 down-regulation seems to occur in early steps of SCC development, with IRF6 already being lower in actinic keratosis, which is considered to be an in situ SCC (Fig. S1*A*).

A strong down-regulation of IRF6 protein expression was observed in cancer cell lines derived from different epithelia, including the esophageal SCC cell lines TE1 and TE13, the epidermoid SCC A431, and the breast cancer cell line MDA-MB231 (Fig. 1*C*), suggesting that IRF6 down-regulation is a common feature of primary SCCs and SCC cell lines.

Author contributions: S.C., M.K., and A.C. designed research; E.B., G.S., F.M., B.M., V.P., and S.G. performed research; E.B., P.D.D.M., F.D.N., F.G., T.C., G.P., L.G., M.F., G.B., and A.C. analyzed data; and E.B., M.K., and A.C. wrote the paper.

The authors declare no conflict of interest.

[1]E.B., G.S., F.M., and B.M. contributed equally to this work.

[2]To whom correspondence may be addressed. E-mail: mkarin@ucsd.edu or antonio.costanzo@uniroma2.it.

This article contains supporting information online at www.pnas.org/lookup/suppl/doi:10.1073/pnas.1110931108/-/DCSupplemental.

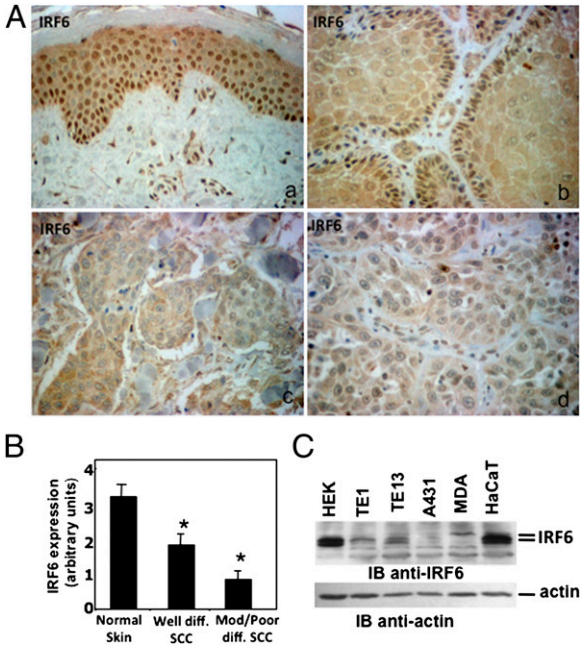

Fig. 1. IRF6 is down-regulated in SCC arising from stratified epithelia. (*A*) A series of 50 tumors and 20 normal tissue samples underwent immunohistochemistry testing with IRF6-specific antibody. *A*, a–d (40× magnification) represent IRF6 staining in normal skin (a), well-differentiated SCC from skin (b), and moderately and poorly differentiated head and neck SCCs (c and d, respectively). (Scale bar: 10 μm.) (*B*) Anti-IRF6 nuclear staining intensity was quantified in three microscopic fields for each tissue section analyzed (50 SCCs and 20 controls) by ImageJ software. The mean staining intensity of positive nuclei was calculated from the tissue arrays and SCC samples containing normal skin stained with anti-IRF6 using ImageJ software after setting the mean cytoplasmic staining intensity as background. The error bars represent 1 SD. *, statistical significance ($P < 0.05$) compared with normal tissue as determined by χ^2 test. IRF6 nuclear staining is strongly reduced in tumors vs. normal epithelium. (*C*) Total protein lysates from normal human keratinocytes (NHKs), esophageal SCC cell lines TE1 and TE13, epidermoid SCC cell line A431, breast cancer cell line MDA-MB-231 (MDA), and immortalized keratinocyte cell line HaCaT underwent IRF6 immunoblotting. Actin immunoblotting was used as a loading control. SCC cell lines displayed strongly reduced IRF6 expression.

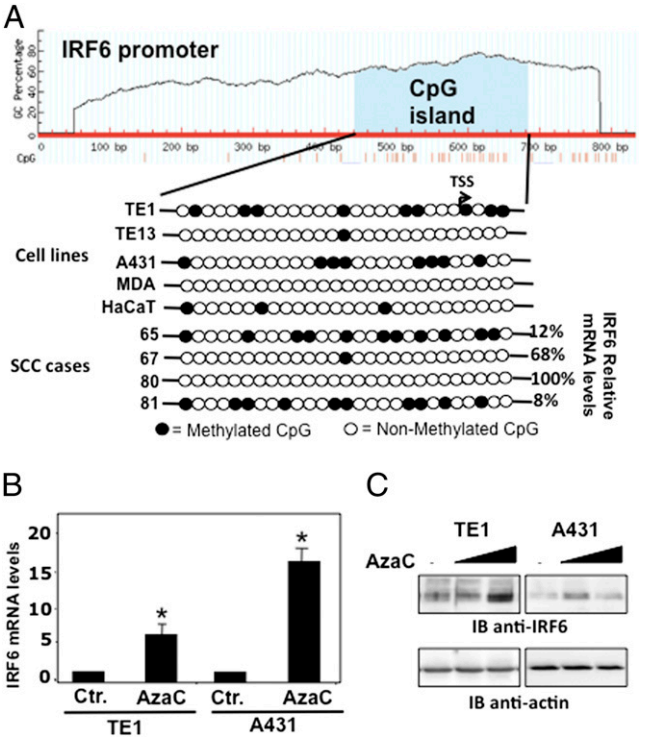

Fig. 2. The *IRF6* gene is epigenetically inactivated by promoter methylation. (*A*) Representation of the CpG island as detected by Meth Primer software (*Top*) (18). A schematic illustration of the position of 5′-methyl cytosines identified by bisulfite sequencing of DNA extracted from the indicated cell lines (*Middle*) or primary SCC (*Bottom*). Relative *IRF6* mRNA expression in primary SCCs is indicated on the right (*Bottom*). *IRF6* promoter is methylated in cell lines and primary SCC showing low IRF6 expression. (*B*) TE1 and A431 cells were mock-treated (Ctr.) or subjected to a 48-h treatment with 5-AzaC (10 μM). After RNA extraction, *IRF6* mRNA was quantified by RT-qPCR. Error bars represent 1 SD. *Statistical significance at $P < 0.05$. (*C*) TE1 and A431 cells showing low IRF6 expression were mock-treated (Ctr.) or subjected to 48-h treatment with 10 or 50 μM 5-AzaC concentrations, and total protein lysates were immunoblots-analyzed with IRF6-specific antibody. Actin was used as a loading control.

***IRF6* Promoter Is Methylated in SCC Cell Lines and Primary Tumors.** Promoter DNA methylation at CpG islands is a common mechanism used by cancer cells to repress expression of tumor suppressor genes (16). To determine whether this mechanism was involved in IRF6 down-regulation, the *IRF6* gene was screened for potential CpG islands using the University of California at Santa Cruz (UCSC) Genome Browser (17). A CpG island located between nucleotides −189 and +10 was found containing 25 CpGs (Fig. 2*A*). The presence of this CpG island was confirmed by adopting a different CpG island searcher program (18). We examined the presence of 5-methyl cytosine within this CpG island in DNA extracted from SCC cell lines, two primary SCCs with *IRF6* mRNA expression and two primary SCCs with low *IRF6* mRNA expression. High levels of methylated CpGs were found in TE1 and A431 cells and the two tumors with low *IRF6* expression (Fig. 2*A*), suggesting that promoter methylation may suppress *IRF6* repression in a subset of SCCs.

To examine the relevance of *IRF6* promoter methylation to regulation of its expression, TE1 and A431 cells were treated with 5-azacytidine (5-AzaC), a DNA methyl transferase inhibitor. *IRF6* expression was evaluated by quantitative RT-PCR (RT-qPCR) and immunoblot analysis. 5-AzaC treatment of primary keratinocytes and SCC cell lines induced *IRF6* expression at both the mRNA and protein levels in the SCC cell lines with the highest *IRF6* promoter methylation (Fig. 2 *B* and *C*), but it had limited effects in other cell lines (Fig. S1*B*). Although other mechanisms may also be involved in IRF6 protein down-regulation, our data suggest that promoter methylation may contribute to repression of *IRF6* transcription in SCC and suggest that IRF6 may act as a tumor suppressor.

Genome-Wide Screening of IRF6 Interacting Sites in Keratinocytes Coupled with Gene Expression Analysis Reveal Direct Antitumoral Target Genes. To identify target genes and regulatory elements that are controlled by IRF6, high-resolution global binding profiles of IRF6 were obtained from normal human keratinocytes (NHK) cell lines established from two unrelated control individuals (wt1 and wt2) by ChIP-seq analysis using an IRF6-specific antibody (IMG-3484). ChIP-seq analysis was performed on cells cultured under differentiating conditions in the presence of 2 mM $CaCl_2$ for 24 h, a time point when IRF6 expression was the highest (12). Gene sequence analysis performed by the peak recognition algorithm of model-based analysis of ChIP-seq (19) gave a highly significant value for 3.983 peaks from two profiles (Fig. 3*A*). These values corresponded to 2,201 genes (Table S1). These peaks were, therefore, considered as a collection of high-fidelity IRF6 binding sites in NHKs. In fact, a set of nine representative binding sites of various peaks, conservation scores, and consensus motif scores

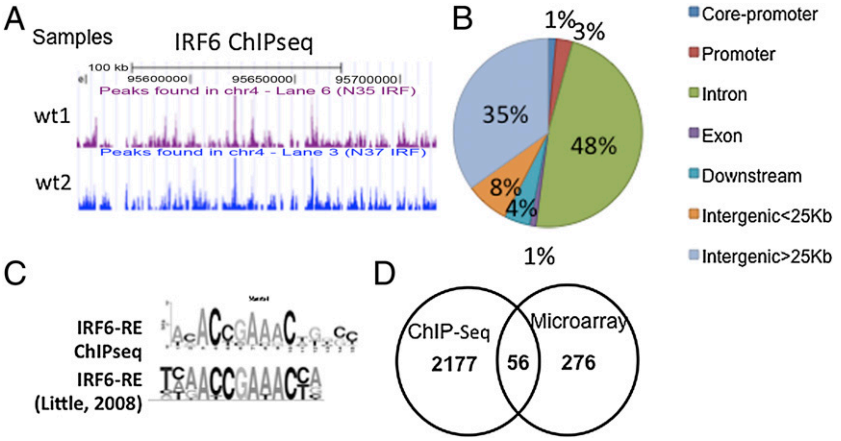

Fig. 3. ChIP-seq analysis of IRF6 binding sites in NHK. (*A*) A screenshot of chromosome 4 using the UCSC genome browser shows similar DNA binding profiles from our ChIP-seq analysis of two normal human primary keratinocyte cell lines (wt1 and wt2) with an IRF6-specific antibody (IMG-3484). (*B*) Distribution of the IRF6 binding site location relative to RefSeq genes. Locations of binding sites are divided into core promoter (1 kb upstream of TSS), promoter [1–5 kb upstream of transcription start site (TSS)], intron (all introns), exon (all exons), downstream (within 5 kb downstream to the last exon), intergenic <25 kb (5–25 kb upstream or 25 kb downstream of last exon), and intergenic >25Kb (all other locations). (*C*) The IRF6 recognition motif was identified by the CisGenome analysis program (*Materials and Methods*) aligned with the previously published IRF6RE (22). (*D*) RNA from Ctr- or IRF6-depleted differentiating NHK was isolated and submitted in triplicates for Affymetrix microarray analysis to identify IRF6-dependent genes. IRF6-bound genes identified in the ChIP dataset (left circle) were overlayed on genes exhibiting IRF6-dependent expression in microarray analyses (right circle); 56 genes were present in both datasets.

were tested with an independent ChIP followed by qPCR analysis (ChIP-qPCR), and all of them were validated (Table S2). This finding reinforced the notion that the IRF6 binding profile was highly reliable. Analyses of peak positions relative to gene locations revealed the distribution shown in Fig. 3*B*.

Standard software (CisGenome) (20) was adopted to distinguish IRF6 responsive elements. A highly significant sequence overrepresentation in genomic regions interacting with IRF6 was observed to have a high level of correspondence but no identity with the published IRF6 binding site (21) (Fig. 3*C*). IRF6 binding genomic regions harboring this consensus were located in genes shown to be important for IRF6 function in craniofacial and bone development [e.g., *TGFBR3* and bone morphogenetic protein 2 (*BMP2*)] (22) and epidermal proliferation/differentiation [e.g., Ovo-like 1(drosophila) (*OVOL1*) and epidermal growth factor receptor (*EGFR*)] (23, 24). The bioinformatic analysis of the top 500 peaks also revealed that activator protein 1 (AP-1) responsive elements were highly represented in IRF6 binding genomic regions (Fig. S1*C*).

To validate whether the identified binding sites represented target genes and regulatory elements relevant to IRF6-associated diseases or cancer, the genes associated with high *P*-value peaks in the Database for Annotation, Visualization and Integrated Discovery (DAVID) database were analyzed (25). Interestingly, gene ontology analysis showed a significant enrichment of peaks related to cell adhesion (p7,40E-12), cell motion (p4,00E-07), cell morphogenesis (p1,50E-06), regulation of cell death (p4,30E-03), and stem cell development (p4,30E-03) (Table S3). In addition, pathway analysis revealed pathways in cancer among the most significant terms (p6,20E-04) (Table S4), confirming a possible involvement of IRF6-regulated genes in the control of cancer development and invasiveness.

To analyze the relevance of IRF6 binding regions and identify additional potential mediators of IRF6 tumor suppressor activity in stratified epithelia, expression profiling on differentiating NHKs silenced for *IRF6* by RNAi (Fig. S1*D*) was performed. Knockdown of *IRF6* in primary human keratinocytes significantly ($P < 0.05$) reduced expression of 269 genes and up-regulated 63 other genes compared with siCtr-transfected NHKs (Table S5). As expected and in agreement with the role of IRF6 in skin development (9, 11), genes down-regulated in IRF6-depleted cells included genes involved in epidermal development and differentiation/keratinization, such as keratins, small proline rich proteins (*SPRR2A* and *SPRR2J*), late cornified envelope genes, *PPARδ*, and *OVOL1* (Table S5). Among up-regulated genes, we found genes involved in controlling keratinocyte proliferation (*NGF*), angiogenesis (*VEGFC*), cell adhesion (integrin-α3, thrombospondin, and *TGF β-induced*), and interaction with extracellular matrix (e.g., tenascinC and matrix metalloproteinase 14) (Table S5). The significance of these findings was confirmed by gene ontology analysis (Table S6); 56 of 332 genes significantly altered in IRF6-depleted keratinocytes were also directly bound by IRF6 in the ChIP-seq experiment (Fig. 3*D* and Table S5). Altogether, these data suggest that IRF6 may directly control genes involved in cell adhesion and epithelial development/proliferation. IRF6 down-regulation leads to impaired differentiation and keratinization (11–13) that correlates with our findings of reduced IRF6 protein levels in less-differentiated SCC samples.

Interestingly, we found *IRF6* itself among the IRF6 target genes (Fig. S2*A*). Three peaks were identified and confirmed by independent ChIP experiments (Fig. S2*B*), two peaks lying in the promoter region and the third peak in the distal region, exactly overlapping the ΔNp63 binding site recently found by Thomason et al. (13). The three binding regions contained IRF6 responsive element (RE) -like sequences showing a high degree of conservation in mammals (Fig. S2*A*). Furthermore, ectopic expression of IRF6 in TE1 cells induced an increase of the endogenous transcript (Fig. S2*C*), suggesting the existence of a positive feedback loop. In addition, *OVOL1* was also found among the genes directly bound by IRF6, and its expression is significantly altered in IRF6-depleted differentiating keratinocytes (Tables S1 and S5). OVOL1 is a repressor of *MYC* transcription that regulates keratinocyte exit from the cell cycle and induction of differentiation, and it is down-regulated in SCCs (4–6). A highly conserved sequence with high homology to the IRF6 consensus was found in a genomic region located 20 kb downstream from the *OVOL1* gene (Fig. 4*A*). An intronic region was also found to bind IRF6 in a ChIP-seq experiment. Independent ChIP and IRF6 knockdown assays performed in proliferating and differentiating keratinocytes confirmed that IRF6 was directly bound to these genomic regions (Fig. 4*B*) and that *OVOL1* transcription was down-regulated in differentiating

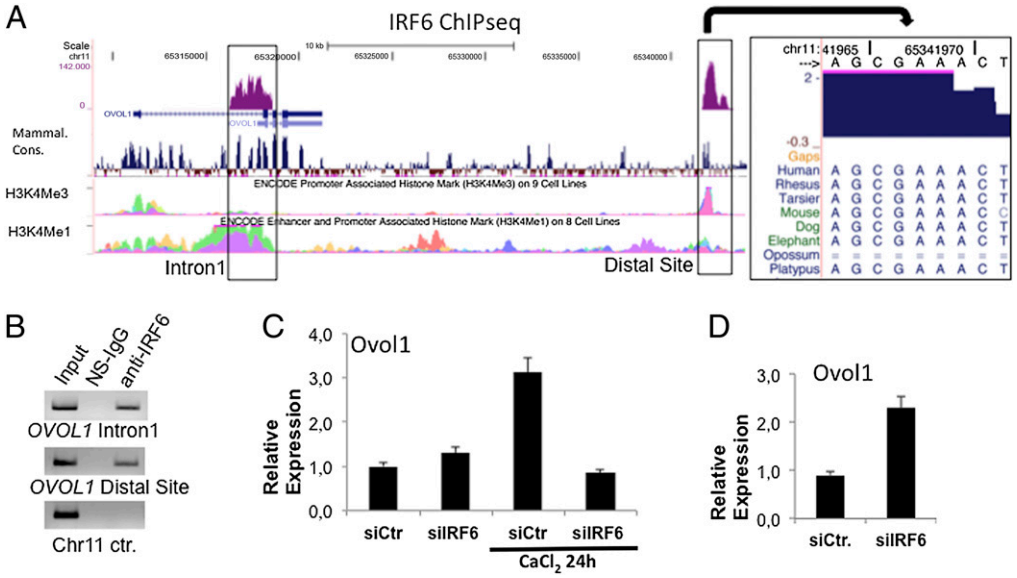

Fig. 4. Characterization of *OVOL1* as an IRF6 target gene. (*A*) The UCSC browser diagram showing the position of ChIP-seq IRF6 peaks near the *OVOL1* gene aligned with mammalian conservation score diagram and H3K4Me3/Me1 diagrams. IRF6 peaks correspond to an increased conservation score and increased H3K4Me3/Me1 regions. The distal site contains a highly conserved sequence closely resembling IRF6RE (right box). (*B*) The independent ChIP assay was performed on differentiating NHK to confirm IRF6 binding to the distal region and the intronic regions of the *OVOL1* gene. A control genomic region on the same chromosome was also amplified (Chr11 ctr). (*C*) NHK were transfected with control siRNA or siIRF6 and left untreated or placed under differentiating conditions (2 mM $CaCl_2$) for 24 h. *IRF6* mRNA levels were evaluated by RT-qPCR. The histogram shows three independent experiments, and error bars represent 1 SD. IRF6 depletion inhibits differentiation-induced *OVOL1* up-regulation. (*D*) TE1 cells were transfected with either control plasmid (pCDNA) or IRF6 expression plasmid (HA-IRF6). mRNA was extracted and subjected to RT-qPCR to quantify *OVOL1* mRNA expression. The histogram represents three independent experiments, and error bars represent 1 SD. Reintroducing IRF6 into TE1 SCC cells induced *OVOL1* expression.

IRF6-depleted cells (Fig. 4*C*). Analysis of OVOL1 expression in TE1 cells confirmed the down-regulation of OVOL1 mRNA in this cell line (Fig. S3*A*), whose *IRF6* promoter region is methylated. Ectopic expression of IRF6 enhanced OVOL1 expression in these cells (Fig. 4*D*).

***IRF6* Regulates Cancer Cell Proliferative Potential in SCCs.** Bypass of oncogene-induced senescence (OIS) is an early step in the process of neoplastic transformation (26). Our observation of early down-regulation of IRF6 in SCC progression (Fig. S1*A*) and the recent discovery that ΔNp63 plays a critical role in inducing bypass of OIS (26) prompted us to analyze the role of IRF6 in regulating this early event. To this aim, we transduced primary human keratinocytes with different combinations of retroviruses expressing an activated form of H-Ras (RasV12), ΔNp63α, or IRF6 (Fig. S3*B*). Colonies were grown for 21 d, counted, and stained for the senescence-associated marker β-galactosidase (SAβ-gal). As expected, ΔNp63 increased the size and number of colonies induced by RasV12 and reduced the number of SAβ-gal–positive cells. IRF6 expression in RasV12/ΔNp63-transcued cells abolished the ability of ΔNp63 to promote colony growth of RasV12-expressing cells and promoted cell senescence (Fig. 5*A*), suggesting that it can neutralize the oncogenic function of ΔNp63.

Our previous identification of IRF6 role in regulation of keratinocyte proliferative potential (12) led us to examine whether IRF6 may also regulate the proliferative potential of cancer cells. To address this question, we assayed clonogenicity of TE1 cells after ectopic expression of IRF6 and observed a dose-dependent reduction in the number and size of colonies arising from IRF6-expressing cells (Fig. 5*B*), thus confirming the role of IRF6 in controlling SCC cell proliferation.

IRF6 Down-Regulation Promotes SCC Invasiveness. The malignant behavior of cancer cells depends largely on their proliferative, invasive, and metastatic activities (27, 28). Invasive and metastatic activities are closely associated with cell to cell and cell to extracellular matrix adhesion as well as with genes involved in wound healing (29, 30). The observations of a cell adhesion signature in ChIP-seq experiment and wound healing in IRF6-depleted cells prompted us to verify whether IRF6 down-regulation may affect the ability of cancer cells to invade surrounding tissues.

TE13 cells were transfected with control or IRF6-specific siRNA and plated on matrigel-coated chambers. IRF6 depletion by siRNA transfection induced strong down-regulation of endogenous IRF6 protein levels (Fig. S3*C*). After cultivating the cells for 18 h, we observed a significant increase in the migration of siIRF6 transfected cells (Fig. 5*D*) that was further enhanced by TGF-β1 treatment. These data are in accordance with the observation of lower IRF6 expression in invasive SCCs and suggest that down-regulation of IRF6 by promoter methylation may confer changes associated with SCC progression.

Discussion

Progression of a tumor from an in situ carcinoma to an invasive and metastatic state depends on genetic and epigenetic changes that alter gene expression and lead to acquisition of new malignant functions by the cancer cell. DNA methylation in tumor suppressor genes occurs frequently and determines transcriptional repression of key mediators of tumor suppression (31). Here, we have exploited the marked reduction in IRF6 expression exhibited by poorly differentiated human SCCs, combined with genome-wide DNA binding and gene profiling, to reveal a previously unrecognized tumor-suppressive function for this developmental factor, whose down-regulation may play a role in SCC invasiveness and proliferation.

We observed reduced IRF6 expression in nuclei of poorly differentiated primary SCCs and SCC cell lines, whose *IRF6* promoter is methylated. IRF6 reexpression after DNA methyl trans-

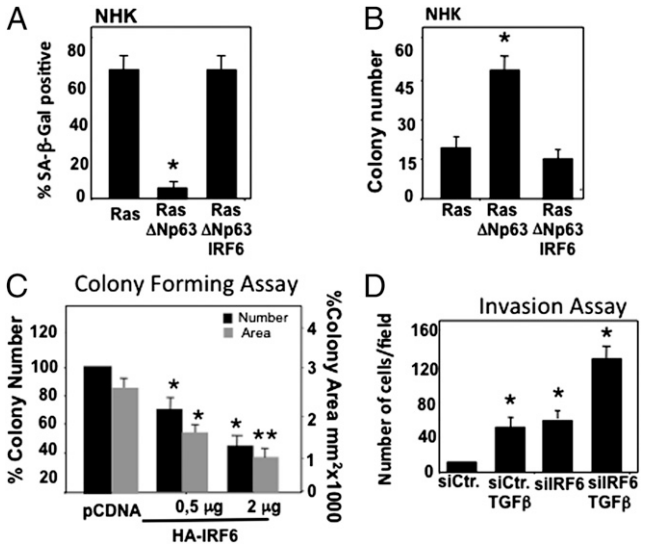

Fig. 5. Analysis of IRF6 tumor suppressive properties. (*A*) Primary human keratinocytes were infected with the indicated retroviral vectors. Cells expressing RasV12 and ΔNp63α continue to proliferate, whereas IRF6 coinfection blocks their growth. SAβ-gal assay shows decreased senescence in cells expressing Ras+ΔNp63α with ectopic IRF6 expression. (*B*) Colony counts of the same cells analyzed in *A*. Error bars represent 1 SD. *, significant differences ($P < 0.05$, two-way unpaired *t* test). (*C*) Colony-forming assays of TE1 cells transfected with control plasmid (pCDNA) or increasing amounts of HA-IRF6–expressing plasmid (IRF6). Cells were cultured in the presence of neomycin (600 μg/mL) 36 h after transfection. Colony-forming efficiency was determined 10 d later and is depicted as percent colony number compared with control-transfected cells (left *y* axis); it represents three independent experiments performed in triplicates. Error bars represent 1 SD. *, significant differences ($P < 0.05$, two-way unpaired *t* test). Relative colony sizes were measured using Image J, and the mean was determined for all colonies ± SD (right *y* axis). **, significant differences ($P < 0.05$, two-tailed Mann–Whitney test of the median). Reexpression of IRF6 in TE1 cells significantly reduced both colony number and size. (*D*) In vitro invasion assays of TE13 cells transfected with the indicated siRNA. The cells were seeded on the upper surface of matrigel-coated transwell chambers and treated with TGFβ1 for 24 h or left untreated. Migrating cells were stained and counted (*Materials and Methods*). Each bar represents a mean of three different experiments performed in triplicates. *, significant differences ($P < 0.05$, two-way unpaired *t* test). The down-regulation of IRF6 in TE13 cells promotes invasiveness that is also enhanced by TGFβ1 treatment.

ferase inhibition suggested that DNA methylation may contribute to IRF6 down-regulation in SCCs. To identify the mechanisms underlying IRF6 tumor suppressor activities, we identified IRF6 binding regions in the human keratinocyte genome by ChIP-seq. This experiment was performed at the onset of keratinocyte terminal differentiation induced in culture by $CaCl_2$ when IRF6 nuclear expression is highest. We observed that direct IRF6 targets include genes involved in cell adhesion and proliferation. Pathway analysis revealed transendothelial migration and pathways in cancer as highly significant terms, further suggesting a role for IRF6 in cancer development and progression. Interestingly, we also found direct binding of IRF6 to three different regions upstream from its own gene, one of which is the same genomic region that controls *IRF6* transcription and is bound by ΔNp63 in proliferating keratinocytes (13). Our observation of increased *IRF6* endogenous transcripts induced by ectopic expression of IRF6 suggests the existence of a positive feedback loop, where IRF6 itself may replace ΔNp63 to keep its own transcription high in differentiating keratinocytes when ΔNp63 is progressively down-regulated (12).

We coupled ChIP-seq analysis with gene expression analysis in IRF6-depleted differentiating keratinocytes and identified a subset of genes whose transcription depends on the direct binding of IRF6. Most of these genes are involved in ectoderm development, keratinocyte proliferation/differentiation switch, and cell–cell contact. Among these functions, we identified the *MYC* repressor *OVOL1* as an IRF6-dependent gene.

This finding is of particular interest, because OVOL1 is a key mediator of IKKα antiproliferative activity in keratinocytes and during SCC progression (4, 5). As stated in the Introduction, *Ikkα*- and *Irf6*-deficient mice display similar developmental phenotypes and epidermal hyperproliferation (11, 13, 14). Therefore, *OVOL1* may represent a common target gene contributing at least in part to this phenotype.

To test the functional effects of IRF6 deficiency on SCC behavior, we performed in vitro invasion and colony formation assays in IRF6-depleted SCC cells. In agreement with the identification of cell adhesion and motility genes as IRF6 targets, we observed strong potentiation of SCC invasive behavior after IRF6 depletion that was further enhanced by TGFβ treatment, suggesting a role for IRF6 as an inhibitor of cell migration and invasion. We explored the role of IRF6 in control of the proliferative potential of keratinocytes that are subjected to oncogenic stress and in cancer cells. Our previous findings indicated that exogenous expression of IRF6 in primary keratinocytes reduced the number of putative stem cell-originating colonies (holoclones) (12). Here, we show that IRF6 can suppress cancer cell growth at both early and late stages of cell transformation. IRF6 restores OIS and inhibits growth of keratinocytes that, because of coexpression of RasV12 and ΔNp63, are expected to bypass senescence. Reexpression of IRF6 in SCC cells harboring a methylated *IRF6* promoter reduces their colony-forming ability and increases the number of small colonies, indicating a negative effect on cancer cell proliferation. These findings are particularly interesting in light of the identification of *OVOL1* as an IRF6 direct target gene. Indeed, OVOL1 was reported to be a major player in determining the exit of keratinocytes from the progenitor cell compartment (23, 24). It is, therefore, tempting to speculate that IRF6 deficiency in SCC may increase the number of stem-like cells.

In conclusion, our study identifies *IRF6* as a potential tumor suppressor gene in SCC acting on a gene network that contributes to the regulation of cancer cell invasiveness and proliferation.

Materials and Methods

Tumor Samples and Immunohistochemistry. Human normal tissues and cutaneous SCC samples came from SuperBioChip (skin cancer array CX1). Sections from the tissue array were formalin-fixed, paraffin-embedded, and pathologically confirmed. Sections were stained with anti-IRF6 (H00003664-B01; Abnova) and an avidin-biotinperoxidase technique by using 3,3′-diaminobenzidine as a substrate (DAKO). Details about the immunohistochemistry and semiquantitative digital image analysis to determine the intensity of IRF6 expression are provided in *SI Materials and Methods*.

Cell Culture. Cell lines used in this study were TE, TE13, MDA-MB-231, A431, HaCaT, and NHK. Cells were grown using standard culture techniques as described previously (13). Details on cell culture are provided in *SI Materials and Methods*.

ChIP and ChIP-Seq. Human primary keratinocytes differentiated for 24 h with $CaCl_2$ were used for ChIP and ChIP-seq analysis. Cells were cross-linked with 1% formaldehyde for 10 min, and chromatin was sonicated using a Sonic Ruptor 250 (Omni International) eight times for 4 min at 50% power on ice. IRF6 antibody IMG-3484 (Imgenex) was used in ChIP-PCR and ChIP-seq analyses. ChIP experiments were performed as described in *SI Materials and Methods*. The sample preparation for sequencing was performed according to the manufacturer's instructions, and data were obtained using an Illumina Genome Analyzer II.

DNA Methylation. DNA was extracted from TE1, TE13, A431, MDA-MB, HaCaT, and NHK by the PureLink Genomic DNA Mini Kit (Invitrogen) according to the manufacturer's instructions. DNA was modified using the Methylamp DNA Modification Kit (Epigentek) as described in the manifacturer's protocol. PCR was performed with the specific primers for methylated DNA that are listed in *SI Materials and Methods*.

The PCR products obtained were subjected to direct sequencing on both strands.

Cell Invasion Assay. The cell invasion assay was performed using a 24-well Transwell chamber (Costar) as previously described (32). Details are provided in *SI Materials and Methods*.

ACKNOWLEDGMENTS. M.K. is an American Cancer Society Research Professor. This work was supported by National Institutes of Health Grant AI043477 (to M.K.) and grants from Associazione Italiana per la Ricerca sul Cancro (no. 5633) (Italy) and Fondo per gli Investimenti della Ricerca di Base-Ideas (FIRB-IDEAS) (to A.C.).

1. Hanahan D, Weinberg RA (2000) The hallmarks of cancer. *Cell* 100:57–70.
2. Akhurst RJ, Balmain A (1999) Genetic events and the role of TGF beta in epithelial tumour progression. *J Pathol* 187:82–90.
3. Mangan PR, et al. (2006) Transforming growth factor-β induces development of the T (H)17 lineage. *Nature* 441:231–234.
4. Descargues P, Sil AK, Karin M (2008) IKKalpha, a critical regulator of epidermal differentiation and a suppressor of skin cancer. *EMBO J* 27:2639–2647.
5. Descargues P, et al. (2008) IKKalpha is a critical coregulator of a Smad4-independent TGFbeta-Smad2/3 signaling pathway that controls keratinocyte differentiation. *Proc Natl Acad Sci USA* 105:2487–2492.
6. Marinari B, et al. (2008) The tumor suppressor activity of IKKalpha in stratified epithelia is exerted in part via the TGF-beta antiproliferative pathway. *Proc Natl Acad Sci USA* 105:17091–17096.
7. Liu B, et al. (2006) A critical role for I kappaB kinase alpha in the development of human and mouse squamous cell carcinomas. *Proc Natl Acad Sci USA* 103: 17202–17207.
8. Savitsky D, Tamura T, Yanai H, Taniguchi T (2010) Regulation of immunity and oncogenesis by the IRF transcription factor family. *Cancer Immunol Immunother* 59: 489–510.
9. Ingraham CR, et al. (2006) Abnormal skin, limb and craniofacial morphogenesis in mice deficient for interferon regulatory factor 6 (Irf6). *Nat Genet* 38:1335–1340.
10. Kondo S, et al. (2002) Mutations in IRF6 cause Van der Woude and popliteal pterygium syndromes. *Nat Genet* 32:285–289.
11. Richardson RJ, et al. (2006) Irf6 is a key determinant of the keratinocyte proliferation-differentiation switch. *Nat Genet* 38:1329–1334.
12. Moretti F, et al. (2010) A regulatory feedback loop involving p63 and IRF6 links the pathogenesis of 2 genetically different human ectodermal dysplasias. *J Clin Invest* 120:1570–1577.
13. Thomason HA, et al. (2010) Cooperation between the transcription factors p63 and IRF6 is essential to prevent cleft palate in mice. *J Clin Invest* 120:1561–1569.
14. Hu Y, et al. (1999) Abnormal morphogenesis but intact IKK activation in mice lacking the IKKalpha subunit of IkappaB kinase. *Science* 284:316–320.
15. Hu Y, et al. (2001) IKKalpha controls formation of the epidermis independently of NF-kappaB. *Nature* 410:710–714.
16. Jones PA, Laird PW (1999) Cancer epigenetics comes of age. *Nat Genet* 21:163–167.
17. Fujita PA, et al. (2010) The UCSC Genome Browser database: Update 2011. *Nucleic Acids Res* 39:D876–D882.
18. Li LC, Dahiya R (2002) MethPrimer: Designing primers for methylation PCRs. *Bioinformatics* 18:1427–1431.
19. Zhang Y, et al. (2008) Model-based analysis of ChIP-Seq (MACS). *Genome Biol* 9: R137. 1–9.
20. Ji H, et al. (2008) An integrated software system for analyzing ChIP-chip and ChIP-seq data. *Nat Biotechnol* 26:1293–1300.
21. Little HJ, et al. (2009) Missense mutations that cause Van der Woude syndrome and popliteal pterygium syndrome affect the DNA-binding and transcriptional activation functions of IRF6. *Hum Mol Genet* 18:535–545.
22. Iwata J, et al. (2010) Transforming growth factor-beta regulates basal transcriptional regulatory machinery to control cell proliferation and differentiation in cranial neural crest-derived osteoprogenitor cells. *J Biol Chem* 285:4975–4982.
23. Nair M, et al. (2006) Ovol1 regulates the growth arrest of embryonic epidermal progenitor cells and represses c-myc transcription. *J Cell Biol* 173:253–264.
24. Teng A, Nair M, Wells J, Segre JA, Dai X (2007) Strain-dependent perinatal lethality of Ovol1-deficient mice and identification of Ovol2 as a downstream target of Ovol1 in skin epidermis. *Biochim Biophys Acta* 1772:89–95.
25. Huang da W, Sherman BT, Lempicki RA (2009) Systematic and integrative analysis of large gene lists using DAVID bioinformatics resources. *Nat Protoc* 4:44–57.
26. Keyes WM, et al. (2011) ΔNp63α is an oncogene that targets chromatin remodeler Lsh to drive skin stem cell proliferation and tumorigenesis. *Cell Stem Cell* 8:164–176.
27. Michelson S, Leith JT (1996) Host response in tumor growth and progression. *Invasion Metastasis* 16:235–246.
28. Kemperman H, Driessens M, La Rivière G, Meijne AM, Roos E (1994–1995) The role of integrins and integrin activation in liver metastasis. *Invasion Metastasis* 14:98–108.
29. Bussemakers MJ, Schalken JA (1996) The role of cell adhesion molecules and proteases in tumor invasion and metastasis. *World J Urol* 14:151–156.
30. Behrens J (1993) The role of cell adhesion molecules in cancer invasion and metastasis. *Breast Cancer Res Treat* 24:175–184.
31. Kulis M, Esteller M (2010) DNA methylation and cancer. *Adv Genet* 70:27–56.
32. Repesh LA (1989) A new in vitro assay for quantitating tumor cell invasion. *Invasion Metastasis* 9:192–208.